Computational Investigation of RO2 + HO2 and RO2 + RO2 Reactions of Monoterpene Derived First-Generation Peroxy Radicals Leading to Radical Recycling

Iyer, Siddharth

2018-12-13

Iyer , S , Reiman , H , Moller , K H , Rissanen , M P , Kjaergaard , H G & Kurten , T 2018 , ' Computational Investigation of RO2 + HO2 and RO2 + RO2 Reactions of Monoterpene Derived First-Generation Peroxy Radicals Leading to Radical Recycling ' , Journal of Physical Chemistry A , vol. 122 , no. 49 , pp. 9542-9552 . https://doi.org/10.1021/acs.jpca.8b09241

http://hdl.handle.net/10138/307397
https://doi.org/10.1021/acs.jpca.8b09241

acceptedVersion

Computational Investigation of RO_2 + HO_2 and RO_2 + RO_2 Reactions of Monoterpene Derived First-Generation Peroxy Radicals Leading to Radical Recycling

Journal:	*The Journal of Physical Chemistry*
Manuscript ID	jp-2018-09241y.R1
Manuscript Type:	Article
Date Submitted by the Author:	n/a
Complete List of Authors:	Iyer, Siddharth; Helsingin Yliopisto, Department of molecular sciences Reiman, Heidi; Helsingin Yliopisto, Department of Chemistry Møller, Kristian; University of Copenhagen, Department of Chemistry Rissanen, Matti; Helsingin Yliopisto, Physics Kjaergaard, Henrik Grum ; Copenhagen University, Chemistry Kurtén, Theo; Helsingin Yliopisto, Department of Chemistry

Computational Investigation of RO_2 + HO_2 and RO_2 + RO_2 Reactions of Monoterpene Derived First-Generation Peroxy Radicals Leading to Radical Recycling

Siddharth Iyer,*,† Heidi Reiman,‡ Kristian H. Møller,¶ Matti P. Rissanen,§ Henrik G. Kjaergaard,¶ and Theo Kurtén*,†

Department of Chemistry and Institute for Atmospheric and Earth System Research (INAR), University of Helsinki, P.O. Box 55, FI-00014, Helsinki, Finland, Department of Chemistry, University of Helsinki, P.O. Box 55, FI-00014, Helsinki, Finland, Department of Chemistry, University of Copenhagen, DK-2100 Copenhagen Ø, Denmark, and Department of Physics and Institute for Atmospheric and Earth System Research (INAR), University of Helsinki, P.O. Box 64, FI-00014, Helsinki, Finland

E-mail: siddharth.iyer@helsinki.fi; theo.kurten@helsinki.fi

Abstract

The oxidation of biogenically emitted volatile organic compounds (BVOC) plays an important role in the formation of secondary organic aerosols (SOA) in the atmosphere. Peroxy radicals (RO_2) are central intermediates in the BVOC oxidation process. Under

*To whom correspondence should be addressed
†University of Helsinki
‡University of Helsinki
¶University of Copenhagen
§University of Helsinki

clean (low-NO_x) conditions, the main bimolecular sink reactions for RO_2 are with the hydroperoxy radical (HO_2) and with other RO_2 radicals. Especially for small RO_2, the RO_2 + HO_2 reaction mainly leads to closed-shell hydroperoxide products. However, there exist other known RO_2 + HO_2 and RO_2 + RO_2 reaction channels that can recycle radicals and oxidants in the atmosphere, potentially leading to lower-volatility products and enhancing SOA formation. In this work, we present a thermodynamic overview of two such reactions: **a)** $RO_2 + HO_2 \rightarrow RO + OH + O_2$ and **b)** $R'O_2 + RO_2 \rightarrow R'O + RO + O_2$ for selected monoterpene + oxidant derived peroxy radicals. The monoterpenes considered are α-pinene, β-pinene, limonene, trans-β-ocimene, and Δ^3-carene. The oxidants considered are the hydroxyl radical (OH), the nitrate radical (NO_3), and ozone (O_3). The reaction Gibbs energies were calculated at the DLPNO-CCSD(T)/def2-QZVPP//ωB97X-D/aug-cc-pVTZ level of theory. All reactions studied here were found to be exergonic in terms of Gibbs energy. Based on a comparison with previous mechanistic studies, we predict that reaction **a** and reaction **b** are likely most important for first-generation peroxy radicals from O_3 oxidation (especially for β-pinene), while less so for most first-generation peroxy radicals from OH and NO_3 oxidation. This is because both reactions are comparatively more exergonic for the O_3 oxidized systems than their OH and NO_3 oxidized counterparts. Our results indicate that bimolecular reactions of certain complex RO_2 may contribute to an increase in radical and oxidant recycling under high HO_2 conditions in the atmosphere, which can potentially enhance SOA formation.

Introduction

Biogenically emitted volatile organic compounds (BVOCs) play a critical role in the formation and growth of atmospheric secondary organic aerosol particles (SOA).[1–4] Once they have grown to sufficient sizes (on the order of ∼100 nm), aerosol particles can affect the Earth's climate both directly, by reflecting solar radiation, and indirectly, by serving as cloud condensation nuclei, and thus modifying cloud properties such as reflectivity and lifetime.[5]

Isoprene (C_5H_8) and monoterpenes, a class of VOCs with the chemical formula $C_{10}H_{16}$, are the most abundant BVOC emissions, accounting for about 69% and 11% of the total global BVOC emission, respectively.[6] These molecules undergo gas-phase reactions with the atmospheric oxidants such as the hydroxyl radical (OH), the nitrate radical (NO_3) and ozone (O_3), forming peroxy radicals (RO_2). Unimolecular reaction pathways of peroxy radicals have recently been demonstrated to be important, especially for the formation of highly oxidized multifunctional organic compounds (HOM) through the process of autoxidation.[4,7] HOMs can have very low volatilities, allowing them to condense and form particles very effectively. Other peroxy radical reaction pathways generally lead to less oxidized and more volatile products, which may nevertheless also contribute to the growth of particulate matter.

α-pinene, β-pinene, limonene, trans-β-ocimene, and Δ^3-carene together account for close to 90% of the global monoterpene emissions.[6] The reaction of monoterpenes with the atmospheric oxidants initiates the process that leads to the formation of a range of products, including the multi-functionalized HOMs. OH initiated oxidation of alkenes can involve either OH radical addition to one of the olefinic carbon atoms, or the abstraction of an aliphatic hydrogen atom. In both cases, the product is an alkyl radical. O_2 can rapidly add to alkyl radicals to form a peroxy radical RO_2.[8] For simple alkyl radicals, a pseudo-unimolecular rate of $\sim 10^7 s^{-1}$ is often assumed for the O_2 + alkyl reaction when the O_2 partial pressure is approximately 0.2 atm.[9,10] NO_3 oxidation also involves addition to one of the olefinic carbon atoms of the alkene (though, in some cases, hydrogen atom abstraction may compete[11,12]), followed by the O_2 addition to the subsequent alkyl radical to form the RO_2. The RO_2 contains an ONO_2 functionality, and closed-shell reaction products retaining this group are commonly called organonitrates. Organonitrates are important in the atmosphere as they can serve as a NO_x (where, x=1,2) reservoir.[13] Ambient measurements have discovered that organonitrates make up a significant fraction of SOA.[14,15]

Ozone oxidation produces peroxy radicals that are structurally different from the peroxy radicals formed following OH or NO_3 oxidation. There are multiple known channels for alkene + ozone reactions. For RO_2 formation, the main channel involves the formation and subsequent decomposition of a vinylhydroperoxide (VHP). Ozonolysis of alkenes (see Figure 2) is initiated by addition of O_3 across the double bond, forming a primary ozonide (POZ). The POZ then rapidly decomposes, forming a Criegee intermediate (CI; a carbonyl oxide) and a carbonyl group. In the case of endocyclic alkenes, such as α-pinene, limonene, and Δ^3-carene, the CI and carbonyl groups remain within the same molecule. For exocyclic, or acyclic alkenes, such as β-pinene and trans-β-ocimene, POZ decomposition leads to fragmentation of the molecule. In the VHP channel, the CI forms a VHP following a 1,4 hydrogen shift (VHP formation may or may not be preceded by collisional stabilization of the CI[16]). The VHP quickly loses an OH, forming a vinoxy radical, which adds O_2 to form the first-generation RO_2.

Monoterpenes (and other alkene VOCs) are thus eventually converted to peroxy radicals by all the main atmospheric oxidants. A myriad of possible unimolecular and bimolecular reactions in the atmosphere determine the fate of these radicals. The chemistry of simpler RO_2 has been explored in detail previously (Orlando et al. 2012[17] and references therein). Over regions with significant anthropogenic emissions, NO can react with RO_2 to produce alkoxy radicals (organonitrate formation is a competing, but generally minor, channel).[17] This is a radical propagating channel, leading also to NO_2, which contributes to the formation of O_3 and ultimately OH (and HO_2).[18] In more pristine conditions that are relatively unaffected by anthropogenic emissions, RO_2 are more likely to react with HO_2 or other RO_2, or undergo unimolecular reactions.

The RO_2 + HO_2 channel becomes relevant in low NO_x conditions, where the lifetime of RO_2 is long enough to react with the HO_2 radical. The RO_2 + HO_2 reaction is usually

assumed to be a radical sink process, forming (mostly) stable hydroperoxides[19] (reaction 1). However, other known RO_2 + HO_2 reaction channels (reaction 2 and reaction 3) can potentially be important and result in radical and oxidant recycling in the atmosphere:

$$RO_2 + HO_2 \rightarrow ROOH + O_2 \quad (1)$$

$$\boldsymbol{RO_2 + HO_2 \rightarrow RO + OH + O_2} \quad (2)$$

$$RO_2 + HO_2 \rightarrow ROH + O_3 \quad (3)$$

Reaction 2 leads to the formation of alkoxy radicals. These radicals can continue oxidation in the atmosphere[20,21] and may lead to products with lower volatilities than the ROOH product of reaction 1. Since the reaction also serves to recycle OH, it can enhance VOC oxidation. Studies of the branching ratios of the two reactions have only been performed for relatively small hydrocarbons (up to 3 carbon atoms).[19,22,23]

The RO_2 + RO_2 reaction has three known channels:

$$R^{'}O_2 + RO_2 \rightarrow R^{'}OH + R^{'}C = O + O_2 \quad (4)$$

$$\boldsymbol{R^{'}O_2 + RO_2 \rightarrow R^{'}O + RO + O_2} \quad (5)$$

$$R^{'}O_2 + RO_2 \rightarrow R^{'}OOR + O_2 \quad (6)$$

Reactions 4 and 6 are both radical termination reactions. Reaction 6 is generally unimportant for small RO_2, but it has been suggested as a mechanism for the lowest-volatility "dimer" reaction products observed in experiments on e.g. monoterpenes.[1,24] Reaction 5 is a radical propagation reaction, and leads to reactive alkoxy radicals analogously to reaction 2. The branching between the competing reaction pathways for both RO_2 + HO_2 and RO_2 + RO_2 reactions are thus important for the radical recycling of the atmosphere.

In this work, we carry out a thermodynamic study of the favorability of the radical-recycling reactions 2 and 5 for a set of the most common monoterpenes and oxidants in the atmosphere. Only the first generation RO_2 is considered, i.e., the RO_2 formed by the first O_2 addition to the alkyl radical following oxidation. Despite this restriction, our study encompasses 83 different RO_2 species, and a total of 3486 possible reactions for reaction 5. We also compute thermodynamic parameters for reaction 3, which has previously been observed for carbonyl-containing acyl peroxy radicals.[19,22,23] It is unlikely that any of the non-acyl peroxy radicals studied here will undergo direct bimolecular reactions with HO_2 to form O_3, as no mechanism has been identified for this in the literature. However, the reaction might conceivably occur in the presence of catalysts, either in the gas-phase via clustering, or in the atmospheric condensed phase. The reaction Gibbs energies for this reaction are provided in Table S1 in the SI. The transition states and associated rates of reactions for the oxidized monoterpenes were not studied in this work because of the large set of reactions and the size of the individual reactants and products considered here.

Methods

The computational methods employed here have been described in detail previously.[8,25,26] The systems studied here possess multiple different isomers, each with a large number of potential conformers. In this context, isomers are defined as compounds with the same chemical elemental composition (and in this case also the same functional groups), but differing in their bonding patterns (i.e. positional isomers). Interconversion of different isomers typically involves the breaking of covalent bonds, and is thus associated with high barriers. Conformers, on the other hand, have identical bonding patterns, and differ only in the three-dimensional arrangement of atoms. Conformers can be interconverted by rotations around torsional angles, which typically have low energy barriers in comparison to reactions breaking and forming

bonds.

The conformer sampling for each isomer was carried out by a systematic conformer search using the MMFF force field,[27–32] followed by single-point energy calculations and geometry optimizations at the B3LYP/6-31+G(d) level of theory.[33–38] Spartan '14 and '16 were used to carry out these computations.[39,40] For the RO_2s and the ROs, the keyword "FFHINT=O_x $\sim\sim$6" (x=radical oxygen atom number as labeled by the Spartan program) was used to denote the radical oxygen and to specify its atom type to "generic divalent O", which was found to yield good results for peroxy radicals.[38,41] Following initial single-point calculations on all the conformers, those within 5 kcal/mol in relative electronic energies of the lowest-energy conformer were optimized at the B3LYP/6-31+G(d) level. Conformers within 2 kcal/mol in relative electronic energy following the optimization were then optimized at the ωB97X-D/aug-cc-pVTZ[42–44] level using the Gaussian 09 program.[45] The calculations were performed using an ultrafine integration grid. Since there were multiple conformers for every reactant and product isomer, the reaction energies were calculated using conformationally averaged Gibbs energies. The equation for calculating the conformationally averaged Gibbs energy, G, is:[46]

$$G = -k_B T \ln\left(e^{-\beta g_0} \sum_k e^{-\beta(g_k - g_0)}\right), \tag{7}$$

where, g_0 is the Gibbs energy of the most energetically favorable conformer, $\beta = 1/k_B T$, g_k is the Gibbs energy of the k^{th} conformer relative to g_0 , k_B is the Boltzmann constant, and T is the temperature. The Gibbs energies for each individual conformer was computed using the standard rigid rotor and harmonic oscillator approximations, with the temperature set to 298.15 K and with a reference pressure of 1 atm (values at different conditions can be computed using the log files provided in a supplementary information file). The conformationally averaged Gibbs energies were then corrected using DLPNO-CCSD(T)/def2-QZVPP single point energies calculated using the ORCA program.[47,48] The DLPNO-CCSD(T)/def2-QZVPP single point calculation was performed on the lowest energy conformer geometry and the

conformationally averaged Gibbs energy was corrected by the difference between the DFT and DLPNO-CCSD(T) electronic energies of the lowest energy conformer. DLPNO stands for domain-based local pair natural orbitals. Instead of canonical delocalized orbitals, the method uses pair natural orbitals that are then localized and classified into domains for sorting and selection of the most important excitations that account for electronic correlation. The DLPNO-CCSD(T) method also differs from corresponding canonical methods when evaluating the triples, using the T_0 approximation which neglects the elements outside the diagonal in the Fock Matrix. This greatly reduces the calculation time. The accuracy of the DLPNO-CCSD(T) method has been tested previously by comparing the DLPNO-CCSD(T) calculated formation enthalpies with accurate formation enthalpies for a set of 113 molecules and found to have a mean absolute error of 1.6 kcal/mol.[49]

Test calculation were performed on small systems with the same functionalities as the molecules studied here to determine the transition state energies for the reaction $RO_2 + HO_2 \rightarrow RO + OH + O_2$ (reaction 2). The transition states were calculated for $CH_2(OH)CH_2OO$ and $CH_2(ONO_2)CH_2OO$ systems (analogous to those formed from OH and NO_3 oxidation) at the CBS/QB3 level,[50] which was used by Hasson et al.[23] for similar systems. These transition states are open-shell singlets and were therefore calculated using unrestricted UCBS-QB3 with the Guess=(mix,always) keyword. This mixes the HOMO and the LUMO so as to destroy the α and β spatial symmetries and requests a new initial guess to be generated at each point in the optimization. The spin contamination in the UHF steps in the CCSD(T) and MP2 calculations in UCBS-QB3 were ∼1.05 before and ∼0.9 after annihilation. The energetics of the intermediate complex of reaction $RO_2' + RO_2 \rightarrow R'O + RO + O_2$ (reaction 5) was studied by optimizing $CH_3CH_2O\cdot\cdots O_2\cdots\cdot OCH_2CH_3$ at the M11/6-31+G(d,p)[35,51–53] level of theory employed in Lee et al.[54]

The reaction Gibbs energies for reactions 2, 3 and 5 were calculated by subtracting the

Gibbs energies of the free products from the Gibbs energies of the free reactants:

$$\Delta G(Reaction\ 2) = [G(RO) + G(OH) + G(O_2)] - [G(RO_2) + G(HO_2)] \quad (8)$$

$$\Delta G(Reaction\ 3) = [G(ROH) + G(O_3)] - [G(RO_2) + G(HO_2)] \quad (9)$$

$$\Delta G(Reaction\ 5) = [G(R'O) + G(RO) + G(O_2)] - [G(R'O_2) + G(RO_2)] \quad (10)$$

The structures of the monoterpenes studied here are shown in Figure 1. For α-pinene and β-pinene, the "-" enantiomers were considered, while for limonene and Δ^3-carene the "+" enantiomers were considered. As the other enantiomers are mirror images, their energetics are identical. For ocimene, trans-β-ocimene was studied as it makes up the majority of the biogenic ocimene emission.[6]

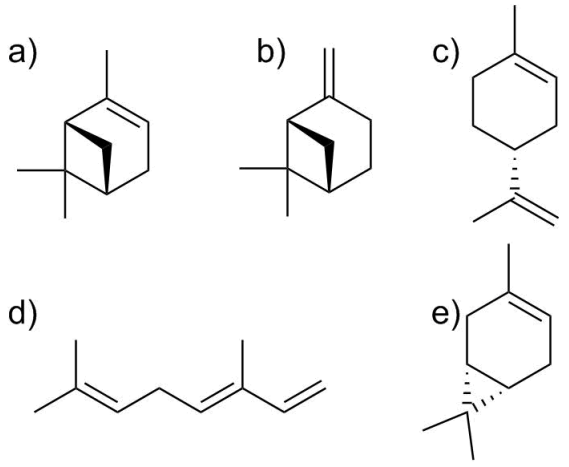

Figure 1: Monoterpene isomers investigated in this study. a) α-pinene, b) β-pinene, c) limonene, d) trans-β-ocimene, and e) Δ^3-carene.

Depending on which olefinic carbon is attacked by the oxidants, multiple isomers of the first-generation RO_2 are possible. For RO_2s from OH and NO_3 oxidation, we generally consider only those isomers formed by addition to the double bond where the initial alkyl radical is formed on the most substituted (tertiary) carbon atom. However, for β-pinene, which has a very limited number of RO_2 isomers from OH and NO_3 oxidation, all first-

generation isomers were calculated to see the effect on the reaction energy. All possible first-generation isomers were also calculated for trans-β-ocimene, including resonance isomers from ozone oxidation. Oxidation via H-abstraction by OH is possible (and can account for a significant fraction of OH oxidation products of monoterpenes according to Rio et al. 2010[55]). However, we decided to limit our study to only oxidation via OH addition as, according to current knowledge, it is still the dominant OH oxidation pathway for monoterpenes.[55,56]

For the ozonolysis reaction, the RO_2 radicals with more than one carbon atom formed via the VHP pathway were considered. The mechanism for trans-β-ocimene is illustrated in Figure 2. For limonene, we only consider ozone attack on the endocyclic double bond, as it has been reported to be 35 times more favorable than the attack on the exocyclic double bond.[57] β-pinene is an exocyclic alkene and thus does not undergo a ring-opening reaction, but instead loses the CH_2 group in the form of formaldehyde (CH_2O) in the POZ decomposition. The CI formed by ozone attack on the terminal double bond of trans-β-ocimene can not form a VHP (as there is no H atom to abstract in a 1,4 H-shift), and this reaction site was thus omitted from our study. Since ozonolysis leads to the breaking of a C=C bond, the RO_2 products of limonene ozonolysis are acyclic, while those of α-pinene and Δ^3-carene have lost their 6-membered rings, but retain their 4- and 3-membered rings, respectively.

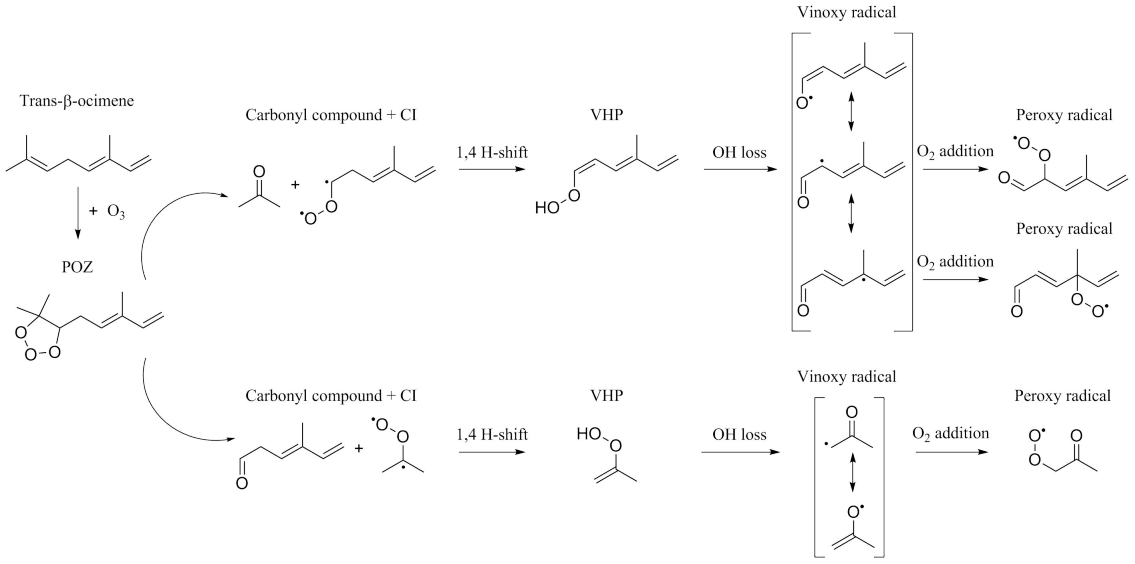

Figure 2: Ozonolysis reaction of trans-β-ocimene over one of the double bonds. The primary ozonide (POZ) can decompose via two possible Criegee intermediate (CI) and carbonyl compound forming channels. The CI forms a vinyl hydroperoxyide (VHP) by a 1,4 hydrogen shift, followed by OH loss to form a vinoxy radical. The vinoxy radical then adds an oxygen molecule, forming a peroxy radical.

Results

$RO_2 + HO_2$ reaction for RO_2 radicals from OH and NO_3 oxidation

The general mechanisms for the initial steps of oxidation via OH and NO_3 addition to double bonds are identical, and the results for the HO_2 reactions with OH and NO_3-derived RO_2 radicals are therefore presented in the same section. The schematic of the lowest energy RO_2 radical isomer is shown in Table 1 for the OH oxidized case and in Table 2 for the NO_3 oxidized case, with the range (maximum-minimum) of Gibbs energies given for the full set of isomers. All reaction Gibbs energies are provided in Tables S4-S8 in the SI. The log files needed to compute them are also provided in the supplementary zip archive.

Table 1: Range of Reaction Gibbs Energies (ΔG) in kcal/mol for Different Isomers For the OH Oxidized Monoterpenes in the $RO_2 + HO_2 \rightarrow RO + OH + O_2$ Reaction

Monoterpene	Isomer[a]	ΔG[b]
α-pinene	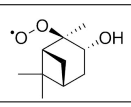	-0.12 to -6.40
β-pinene	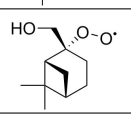	-2.03 to -4.88
Trans-β-ocimene	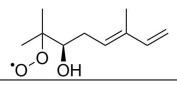	-1.47 to -3.85
Limonene	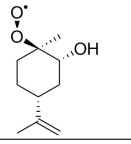	-1.11 to -2.61
Δ^3-carene	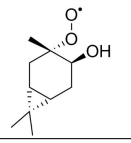	-1.34 to -4.70

[a] Lowest energy RO_2 isomer (in terms of Gibbs energy at 298.15 K).

[b] Gibbs energies (at 298.15 K and 1 atm reference pressure) are conformationally averaged and calculated at the DLPNO-CCSD(T)/def2-QZVPP//ωB97X-D/aug-cc-pVTZ level.

Table 2: Range of Reaction Gibbs Energies (ΔG) in kcal/mol for Different Isomers For the NO_3 Oxidized Monoterpenes in the $RO_2 + HO_2 \rightarrow RO + OH + O_2$ Reaction

Monoterpene	Isomer[a]	ΔG[b]
α-pinene	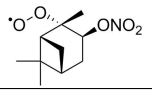	-1.79 to -5.25
β-pinene	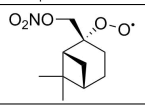	-1.74 to -4.88
Trans-β-ocimene	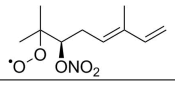	-1.78 to -5.52
Limonene	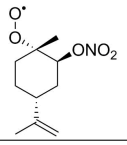	-1.63 to -4.40
Δ^3-carene	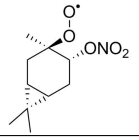	-2.13 to -5.75

[a] Lowest energy RO_2 isomer (in terms of Gibbs energy at 298.15 K).

[b] Gibbs energies (at 298.15 K and 1 atm reference pressure) are conformationally averaged and calculated at the DLPNO-CCSD(T)/def2-QZVPP//ωB97X-D/aug-cc-pVTZ level.

$RO_2 + HO_2$ reaction for RO_2 from ozonolysis

The range (maximum-minimum) of the reaction Gibbs energies for the different isomers of the ozonolysis derived RO_2s are given in Table 3, with the schematic of the lowest energy RO_2 also shown. The ozonolysis of trans-β-ocimene leads to the formation of peroxy radicals with different elemental compositions which are not isomers of each other. Therefore, the reaction energies for each of the different trans-β-ocimene derived RO_2s are shown separately in Table 4.

Table 3: Range of Reaction Gibbs Energies (ΔG) in kcal/mol For Different Isomers for the O_3 Oxidized Monoterpenes in the $RO_2 + HO_2 \rightarrow RO + OH + O_2$ Reaction

Monoterpene	Isomer[a]	ΔG[b]
α-pinene	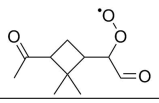	-4.03 to -4.16 (-26.64,-25.42)[c]
β-pinene	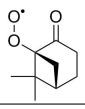	-4.24 to -7.16
Trans-β-ocimene	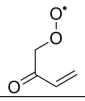	-2.38 to -4.68
Limonene	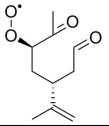	-4.02 to -4.70
Δ^3-carene	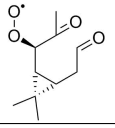	-2.09 to -4.70

[a] Lowest energy RO_2 isomer (in terms of Gibbs energy at 298.15 K).

[b] Gibbs energies (at 298.15 K and 1 atm reference pressure) are conformationally averaged and calculated at the DLPNO-CCSD(T)/def2-QZVPP//ωB97X-D/aug-cc-pVTZ level.

[c] Includes alkoxy ring-breaking step as no alkoxy radical minimum could be found.

Table 4: Reaction Gibbs Energies (ΔG) in kcal/mol for All The Trans-β-Ocimene Ozonolysis Isomers Considered In This Study in the $RO_2 + HO_2 \rightarrow RO + OH + O_2$ Reaction

RO_2	Isomer	ΔG^a
1	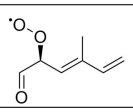	-2.70
2	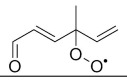	-2.37
3		-4.03
4	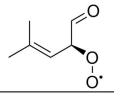	-2.37
5	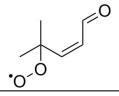	-1.97
6		-4.68

[a] Gibbs energies (at 298.15 K and 1 atm reference pressure) are conformationally averaged and calculated at the DLPNO-CCSD(T)/def2-QZVPP//ωB97X-D/aug-cc-pVTZ level.

The RO_2s from α-pinene ozonolysis with the radical group located on the ring were excluded from the study due to a previously reported ring-breaking reaction that occurs spontaneously upon formation of the RO product,[8] making the alkoxy forming channel significantly exergonic. In this reaction, the alkoxy oxygen forms a carbonyl group, breaking the four-member cyclobutyl ring in the process, forming a second-generation alkyl radical, as shown in Figure 3. Reaction thermodynamics for the other two RO_2s formed in α-pinene ozonolysis are comparable to the other monoterpenes.

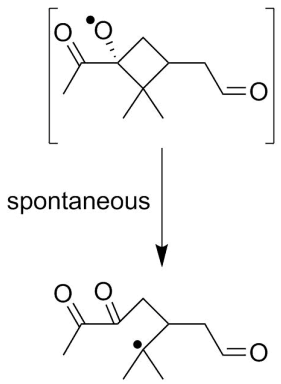

Figure 3: Ring breaking reaction observed during the optimization of the RO product for the most favorable RO_2 isomer product following ozonolysis of α-pinene.

$\mathbf{R'O_2 + RO_2 \rightarrow R'O + RO + O_2}$ reaction

For reaction 5, 83 self-reactions + (83×82)/2 cross-reactions were possible, giving a total of 3486 reactions when all the monoterpene + oxidant combinations were considered. The reaction Gibbs energies varied from a maximum of -2.86 kcal/mol to a minimum of -16.96 kcal/mol. Table 5 shows the reaction Gibbs energies of a select few reactions categorized into reaction energy ranges of 0 to -5, -5 to -10, and -10 to -17 kcal/mol. Reaction Gibbs energy ranges were used to point out important RO_2/RO features that were found to strongly influence the reaction Gibbs energies. The complete set of reaction Gibbs energies is provided as an Excel spreadsheet in the supplementary material.

Table 5: Reaction Gibbs Energies (ΔG) in kcal/mol for Selected $R'O_2 + RO_2 \rightarrow R'O + RO + O_2$ Reactions

Range		Isomer		ΔG^a
		$R'O_2$	RO_2	
0 to -5	**a**	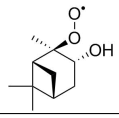	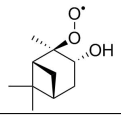	-2.86
	b	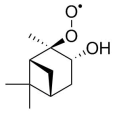	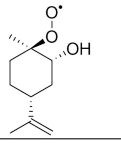	-3.86
	c	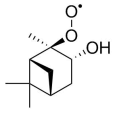	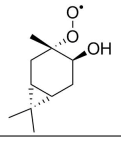	-4.08
-5 to -10	**d**	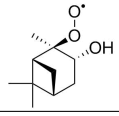	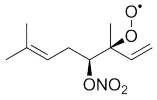	-5.90
	e	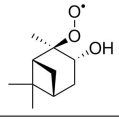	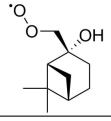	-7.63
	f	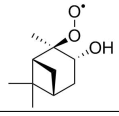	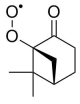	-9.91
-10 to -17	**g**	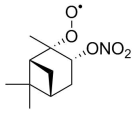	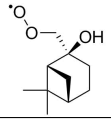	-12.40
	h	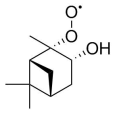	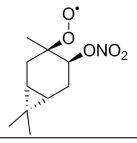	-14.78
	i	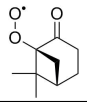	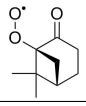	-16.96

[a] Gibbs energies (at 298.15 K and 1 atm reference pressure) are conformationally averaged and calculated at the DLPNO-CCSD(T)/def2-QZVPP//ωB97X-D/aug-cc-pVTZ level.

The reaction Gibbs energies of reaction 5 point to low favorability for the reactions involving the OH-oxidized α-pinene isomer with the RO_2 functional group and OH functional group on the opposite sides of the ring. The first six entries in Table 5 all have this isomer as

the $R'O_2$ reactant to help illustrate how the identity of the other peroxy radical changes the reaction thermodynamics.

Discussion and Atmospheric Implications

All reactions studied here had standard Gibbs energies below 0. However, while important, this is not a sufficient condition for a reaction to be competitive under atmospheric conditions. The atmospheric importance of a reaction depends on its reaction rate. While reaction rates cannot be determined from the thermodynamic parameters reported here, some general guidelines can help illustrate which reactions might be competitive in atmospheric conditions, and which can be ruled out.

Most of the reactions studied here likely involve transition states, or at least reactant complexes or reaction intermediates, which suffer from an entropy penalty compared to the free reactants (or products) due to the loss of translational and rotational degrees of freedom. This is especially important for reaction 2 and reaction 5, where two reactants first combine, and then separate to form three products, with an associated gain in entropy. Our discussion here focuses on parameters computed at 298.15 K. The rates of bimolecular radical reactions in the atmosphere are typically not very temperature-sensitive (as the enthalpy barriers of competitive reaction channels are inevitably fairly close to zero), and the general conclusions drawn here can thus likely be applied to most of the lower troposphere. Thermodynamic parameters at other temperatures can be computed from the data in the log files (provided as a supplementary material zip archive).

$\mathbf{RO_2 + HO_2 \rightarrow RO + OH + O_2}$

The overall entropy gain in reaction 2 translates to a difference of around 9-10 kcal/mol between the reaction enthalpies and the reaction Gibbs energies (computed at the ωB97X-

D/aug-cc-pVTZ level as the thermal contributions to the Gibbs energy are available only at this level). Similarly, the entropy contributions to the Gibbs energies (-TΔS) of the transition states and/or intermediates for reaction 2 must be around 20 kcal/mol higher than those of the products. If the transition states and products were isoenergetic in terms of the enthalpy, a reaction Gibbs energy of 0 kcal/mol would thus imply a barrier of about 20 kcal/mol – making the reaction much too slow to matter in the atmosphere.

In reality, the transition states and separated products are not isoenergetic – either can contain both stabilizing and destabilizing interactions that are lacking in the other. Hasson et al.[23] found that for ethyl peroxy and acetonyl peroxy radicals, the rate-limiting transition states for reaction 2 were 7.5 and 13.7 kcal/mol below the separated products in enthalpies, respectively (the transition states can be lower than the products due to the presence of multiple intermediates or product complexes on the reaction path).

The entropy contribution to the Gibbs energy of the transition state relative to the products, and the stabilization of the transition state due to inter-molecular interactions, were further investigated for reaction 2 by performing test calculations on small systems with the same functionalities as the OH and NO_3 oxidized RO_2 (two-carbon systems $CH_2(OH)CH_2OO$ and $CH_2(ONO_2)CH_2OO$). The analogous system for O_3 oxidation is the acetonyl peroxy radical, which was already studied by Hasson et al.[23] The enthalpies, entropy contributions (-TΔS), and Gibbs energies for key stationary points of the $CH_2(OH)CH_2OO + HO_2 \rightarrow CH_2(OH)CH_2O + OH + O_2$ reaction are shown in Figure 4. Only the rate limiting transition state energy is shown. There are multiple intermediates and transition states between intermediate 2 (INT_2 in Figure 4) and the separated products. Hasson et al.[23] provide the entire reaction pathway for alkyl, acyl, and acetonyl type RO_2s. The transition states for the OH- and NO_3-oxidized systems were found to be 12.4 kcal/mol and 13.2 kcal/mol lower in enthalpies, respectively, than the corresponding free products (these values were calculated

at the same computational level employed in Hasson et al.- CBS-QB3[23]). This is very similar to the value of 13.7 kcal/mol found for the acetonyl peroxy radical, indicating that transition states for all RO_2 + HO_2 reactions studied here are stabilized (in enthalpy, compared to the free products) by roughly similar amounts. The entropy contribution to the Gibbs energy of the transition state relative to the free products was 21.5 and 21.8 kcal/mol for OH- and NO_3-oxidized systems, respectively (and 23.6 kcal/mol for the acetonyl peroxy radical[23]). In terms of Gibbs energy (accounting for both the entropy contribution to the transition state Gibbs energy and the stabilization of the transition state due to favorable intra-molecular interactions) the transition states were thus 9.4, 8.0, and 9.9 kcal/mol above the reactants for the OH-, NO_3, and O_3 oxidized systems, respectively.

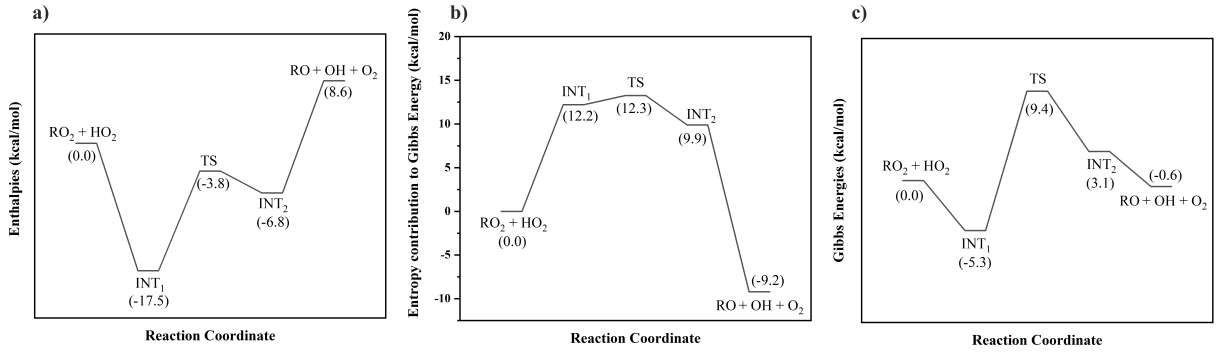

Figure 4: Reaction stationary points for the RO_2 + HO_2 reaction, where the RO_2 = $CH_2(OH)CH_2OO$, in terms of a) enthalpies and c) Gibbs energies. b) shows the entropy contribution (-TΔS at 298.15 K) to the Gibbs energies calculated at the CBS-QB3 level of theory. INT = intermediate, TS = transition state.

The overall rates (including all channels) for RO_2 + HO_2 reactions are typically on the order of 10^{-11} cm^3 $molecules^{-1}$ s^{-1}, and they typically increase with the size of the RO_2.[58] For a particular reaction channel (such as reaction 2) to be competitive, its rate can thus not be much lower than this. Using elementary transition state theory, a rate of 10^{-11} cm^3 $molecules^{-1}$ s^{-1} corresponds to a Gibbs energy barrier of approximately 5 kcal/mol. Based on our test calculations and Hasson et al.,[23] for the two-carbon systems, the entropy penalty to the Gibbs energy of the transition states is about 22 kcal/mol relative to the products, while

the TS enthalpies are about 13 kcal/mol below the products of reaction 2 due to favorable intra-molecular interactions. Thus, for the Gibbs energy barrier to be 5 kcal/mol or less, the Gibbs energy of reaction 2 should not be higher than -4 kcal/mol. While our test systems have the same functional groups as the molecules in this study, the calculated -TΔS and enthalpic contributions to the transition state Gibbs energy of reaction 2 cannot be assumed to be directly applicable to all the monoterpene derived reactants and products studied here. However, test calculations on one α-pinene derived RO_2 (see section S3 in the SI) indicate that our "rule of thumb" may be reasonably valid also for larger systems, and can thus be helpful in gauging what reactions are likely to be competitive. We can conclude therefore that any example of reaction 2 with an overall Gibbs energy much above -4 kcal/mol is unlikely to be competitive in the atmosphere. As seen from tables 1 to 4, this includes most (though not all) of the OH and NO_3 derived 1st generation RO_2, and some of the RO_2 from O_3 oxidation of trans-β-ocimene and Δ^3-carene. On the other hand, for each monoterpene + oxidant combination except limonene + OH, at least one isomer can be found for which the Gibbs energy of reaction 2 is around or below -4 kcal/mol.

Intra-molecular hydrogen bonds generally lower the Gibbs energy of molecules. A lower reactant RO_2 energy (for example, due to hydrogen bonding) will increase the reaction energy, while a lower product RO energy will decrease the reaction energy. The alkoxy RO product from the OH-oxidized RO_2 isomer for α-pinene shown in Table 1 has the alkoxy oxygen on the opposite side of the ring to the OH-group and is therefore unable to form an intra-molecular hydrogen bond. The RO_2 group in the reactant is more flexible and is able to form a weak hydrogen bond with the OH group. This results in a high reaction 2 Gibbs energy of -0.12 kcal/mol. The reaction Gibbs energy corresponding to the reactant RO_2 isomer where the OH-group is on the same side as the peroxy radical is significantly more exergonic (-6.40 kcal/mol) due to a strong intra-molecular hydrogen bond between the alkoxy oxygen and the OH group in the product, and a relatively weaker interaction between the RO_2 group and

the OH group in the reactant. Figure 5 shows the two alkoxy radical isomers schematically. Isomer b in the figure can form an intra-molecular hydrogen bond between the alkoxy-oxygen and the OH-group and is consequently about 5 kcal/mol lower in Gibbs energy than the RO isomer **a**.

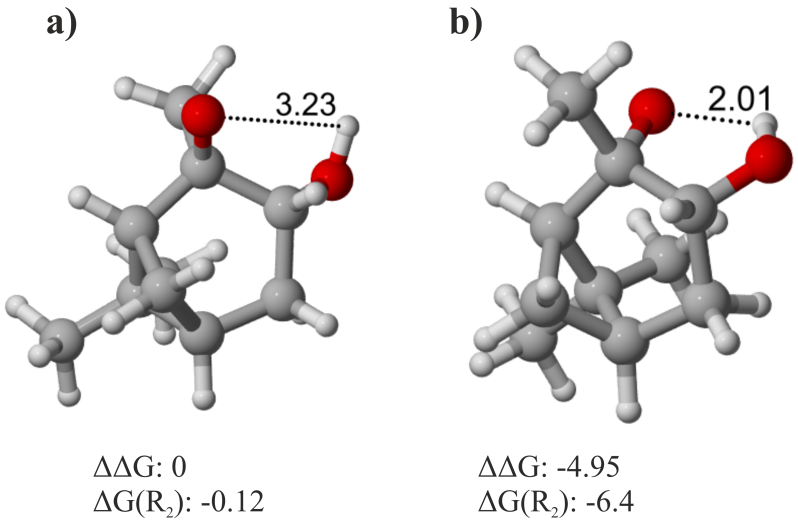

Figure 5: Alkoxy products of OH-oxidized α-pinene a) OH down, O up, b) OH down, O down. $\Delta\Delta$G denotes the relative Gibbs energies of the alkoxy isomers and ΔG(R_2) is the Gibbs energy of reaction 2 producing this product. All values are in kcal/mol.

In the case of OH-derived RO_2, the reaction rate may ultimately be controlled by the degree of hydrogen bonding stabilization of the transition states, which cannot be directly deduced from the overall reaction energies. In other words, our "rule of thumb" of an overall reaction Gibbs energy not much above -4 kcal/mol being necessary for an efficient reaction 2 may have the largest uncertainty for the OH-oxidized cases.

In the case of NO_3 oxidation, the difference between the reaction Gibbs energies of different isomers for each monoterpene is controlled mainly by the stability of the reactant RO_2, as the differences in Gibbs energies between the RO_2 is larger than the difference in Gibbs energies of the corresponding RO. For trans-β-ocimene, the most energetically favorable RO_2 isomer (shown in Table 2) was 3.68 kcal/mol lower in Gibbs energy than the next best RO_2

isomer. This showed in the reaction Gibbs energies for reaction 2, where the most favorable RO_2 isomer lead to the highest (least negative) reaction Gibbs energy. The RO_2 isomer that has the O_2 and ONO_2 functional groups in opposite positions compared to the lowest Gibbs energy RO_2 isomer had a relative Gibbs energy of 4.77 kcal/mol and a reaction 2 Gibbs energy of -5.52 kcal/mol. The two isomers are shown schematically in Figure 6. Similarly, the Δ_3-carene NO_3 oxidized RO_2 isomer that is 2.60 kcal/mol (**b** in Figure 7) higher in Gibbs energy than the most energetically favorable isomer (**a** in Figure 7) has a reaction 2 Gibbs energy of -5.75 kcal/mol compared to -2.13 kcal/mol for the latter.

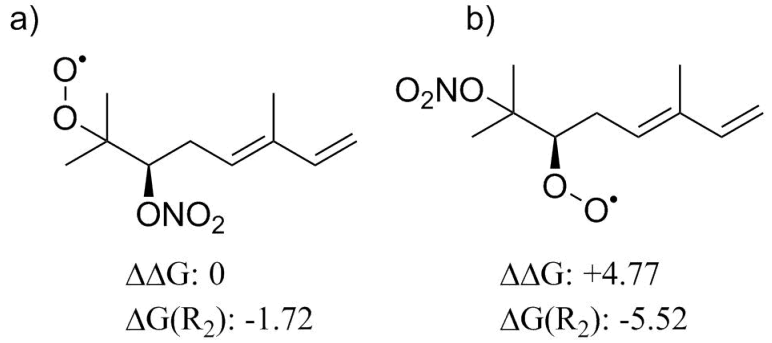

Figure 6: Two of the RO_2 isomers for NO_3 oxidized trans-β-ocimene that were studied. $\Delta\Delta$G denotes the relative Gibbs energy in kcal/mol. **a)** Is the most energetically favorable RO_2 isomer, while **b)** is an isomer that is 4.77 kcal/mol higher in Gibbs energy. ΔG(R_2) is the Gibbs energy of reaction 2 involving this reactant.

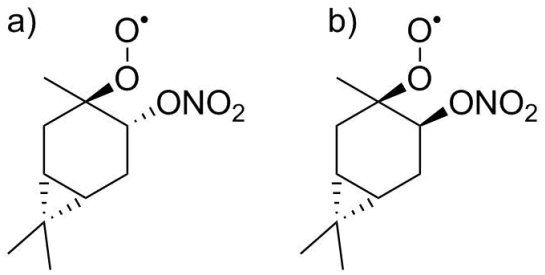

Figure 7: Two of the RO_2 isomers for NO_3 oxidized Δ_3-carene that were studied. $\Delta\Delta G$ denotes the relative Gibbs energy in kcal/mol. **a)** Is the most energetically favorable RO_2 isomer and **b)** is an isomer that is 3.25 kcal/mol higher in Gibbs energy. $\Delta G(R_2)$ is the Gibbs energy of reaction 2 involving this reactant.

The Gibbs energies of reaction 2 for the O_3 oxidized systems were on average slightly lower than for the OH and NO_3-oxidized cases. The variation of Gibbs energies (both for different RO_2 isomers from the same monoterpene, and between monoterpenes) was also generally slightly smaller, possibly due to weaker direct interactions between the carbonyl group and the radical centers compared to the ONO_2 or OH cases. Crucially, most RO_2 isomers derived from O_3 oxidation of monoterpenes had Gibbs energies just around or below -4 kcal/mol for reaction 2, implying that they could be competitive in the atmosphere. The main exceptions to this trend are some RO_2 isomers from trans-β-ocimene and Δ^3-carene ozonolysis, which have reaction Gibbs energies between -2 and -3 kcal/mol, and one of the RO_2 isomers from β-pinene ozonolysis, which has an anomalously low reaction Gibbs energy of -7.16 kcal/mol. This last isomer has the RO_2 (and subsequent RO) group located on a tertiary carbon atom, leading to an exceptionally low energy for the RO product. While spontaneous breaking of the cyclo-butyl ring by the oxy-radical on the tertiary carbon was expected (and was observed at the lower-level B3LYP/6-31+G* optimization), a direct optimization at the higher ωB97X-D/aug-cc-pVTZ level found an alkoxy radical minimum (note that the ring-breaking reaction is still likely to have a low barrier, and occur before any other reaction in atmospheric conditions). The three RO isomers of ozone oxidized β-pinene along with the

difference in relative Gibbs energies are shown in Figure 8. It should be noted that isomer **a** is unlikely to form in the atmosphere as the initial hydrogen abstraction by the Criegee intermediate required to form the preceding RO_2 has a barrier of 25 kcal/mol.[59]

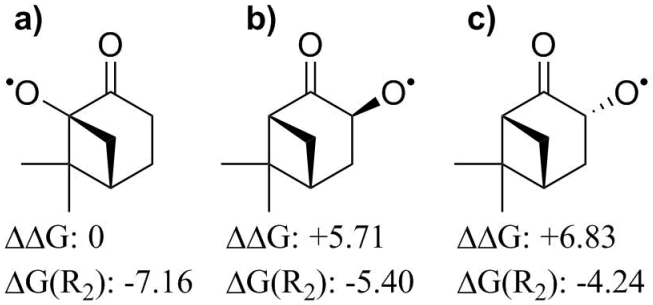

Figure 8: The three RO isomers for O_3 oxidized β-pinene. $\Delta\Delta$G denotes the relative Gibbs energy in kcal/mol. **a)** Is the isomer with the oxy radical on the tertiary carbon atom, while **b)** and **c)** are the isomers with the oxy radical on the secondary carbon atom. ΔG(R_2) is the Gibbs energy of reaction 2 producing this product.

Reaction 3 was found to be consistently exergonic, by -13 to -25 kcal/mol, see Table S1 in the SI for full details. The most favorable reaction Gibbs energies were observed for the isomers where the alcohol product formed an intra-molecular hydrogen bond with the O-atom of the OH, NO_3, and the carbonyl O functional groups from the three different oxidized systems, respectively. If (likely catalytic) kinetically competitive reaction mechanisms exist for reaction 3 also for the non-acyl peroxy radicals studied here, then thermodynamic factors will not prevent the reaction from occurring.

$\mathbf{R'O_2 + RO_2 \rightarrow R'O + RO + O_2}$

The mechanism of reaction 5 is currently uncertain. The most recent and theoretically rigorous computational study by Lee et al.[54] proposes (in agreement with a multireference study by Ghigo et al. from 2003[60]) that all RO_2 + RO_2 reactions proceed via an $RO\cdots O_2\cdots RO$ complex, where the two RO are coupled as a triplet, coupling to the triplet O_2 to give an overall singlet. Branching between the three different pathways (reactions 4, 5 and 6)

is then controlled by a competition between hydrogen abstraction, fragmentation of the complex and intersystem crossing (and subsequent barrierless recombination of the two RO), respectively. The thermodynamic parameters computed here can thus not be used to assess relative probabilities of reaction 5 compared to the two other channels. However, analogous to reaction 2, the $RO\cdot\cdot\cdot O_2\cdot\cdot\cdot RO$ complex also suffers from an entropy penalty to its Gibbs energy compared to the separated products (in terms of the -TΔS contribution to the Gibbs energy at 298 K). For example, the entropy contribution to the Gibbs energy of the $CH_3CH_2O\cdot\cdot\cdot O_2\cdot\cdot\cdot OCH_2CH_3$ complex was found to be 17 kcal/mol relative to the separated products (calculated at M11//6-31+G(d,p) level employed by Lee et al.[54]). Since the entropy penalty to the Gibbs energy of the $RO\cdot\cdot\cdot O_2\cdot\cdot\cdot OR$ complex and the transition state (or states) associated with its formation are likely quite similar (see Figure 4 **b** for the analogous case for reaction 2), the overall RO_2 + RO_2 reaction is thus associated with a Gibbs energy barrier around 17 kcal/mol higher than the reaction Gibbs energy computed here, plus or minus any stabilizing or destabilizing enthalpic contributions, for example from H-bonding or bond-breaking (respectively). Lee et al.[54] suggest (based on CCSD(T) energy corrections) that the rate-limiting transition state for the CH_3CH_2OO + CH_3CH_2OO reaction is almost 13 kcal/mol above the $RO\cdot\cdot\cdot O_2\cdot\cdot\cdot OR$ complex in enthalpy. This would lead to negligibly low overall reaction rates for the gas-phase CH_3CH_2OO + CH_3CH_2OO reaction, in disagreement with observations.[17] CASPT2 calculations by Ghigo et al.[60] for the CH_3OO + CH_3OO system suggest that the rate-limiting transition state is less than 2 kcal/mol above the complex in enthalpy, leading to much better agreement with experiments. Here, we use computed properties for a few model $RO\cdot\cdot\cdot O_2\cdot\cdot\cdot OR$ and $RO\cdot\cdot\cdot OR$ complexes, together with our computed overall reaction Gibbs energies, to estimate lower limits for the barrier heights for the RO_2 + RO_2 reactions. If the rate-limiting transition states are much higher in enthalpy than the $RO\cdot\cdot\cdot O_2\cdot\cdot\cdot OR$ complex, the barriers would be correspondingly higher. However, as long as the reaction proceeds via the $RO\cdot\cdot\cdot O_2\cdot\cdot\cdot OR$ complex, the rate-limiting barrier cannot not be lower than the free energy of the complex.

If we consider that the stabilization of the RO$\cdots$O$_2\cdots$OR complex is mostly from the favorable interaction of the two RO, we can estimate this stabilization by looking at the binding energy of RO$\cdots$RO. We considered a simple two-carbon model ROs for each of the OH-, NO_3, and O_3-oxidized system. The calculation was done for an overall triplet state, as the Lee et al.[54] mechanism indicates the two RO are initially coupled as a triplet (and ROOR formation from two RO likely occurs spontaneously on the singlet surface). The binding enthalpy (at the DLPNO/def2-QZVPP//ωB97X-D/aug-cc-pVTZ level of theory) for the OH-, NO_3- and O_3 oxidized RO$\cdots$RO is 4.4, 3.9 and 2.7 kcal/mol, respectively. Considering an entropy penalty to the transition state Gibbs energy of around 17 kcal/mol, a stabilization of around 4 kcal/mol would mean that the rate limiting transition state (or intermediate) for reaction 5 is at least around 13 kcal/mol above the separated products. For example, for a reaction Gibbs energy of around -10 kcal/mol (implying that the products are 10 kcal/mol below the reactants), the transition state would then be about 3 kcal/mol in Gibbs energy above the reactants.

The reaction Gibbs energies of reaction 5 showed that the reaction was less favorable when one of the reacting peroxy radicals was the OH-oxidized α-pinene isomer with the RO_2 functional group and the OH functional group on the opposite sides of the ring (see rows **a** to **f** in Table 5). This is due to the previously discussed stabilization of the OH-oxidized α-pinene RO_2 by a weak H-bond between the hydrogen atom of the OH group and the RO_2 group and the absence of such an interaction in the corresponding RO product (see Figure 9). For the reactions in the range of -5 to -10 kcal/mol, the lowering of the OH-oxidized α-pinene peroxy radical isomer due to the interaction between the RO_2 and OH groups were compensated by the relatively high energies of the second RO_2 reactant in the reaction. The NO_3-oxidized trans-β-ocimene RO_2 isomer in row **d** in Table 5 is 4.4 kcal/mol higher in Gibbs energy compared to the most favorable NO_3-oxidized trans-β-ocimene RO_2 isomer.

Similarly, the OH-oxidized β-pinene RO_2 in row **e** in the table has the peroxy radical group on a secondary carbon, and is consequently 1 kcal/mol higher in Gibbs energy relative to the lowest energy OH-oxidized β-pinene RO_2 isomer. While 1 kcal/mol should not significantly affect the overall reaction Gibbs energy on its own, the ΔG is augmented by the low energy of the corresponding RO product of this OH-oxidized β-pinene RO_2 isomer in row **e**, which is the most favorable RO isomer of the four considered in this study. For the third case in this energy range, the ΔG is significantly influenced by the previously discussed low RO Gibbs energy of the O_3-oxidized β-pinene isomer in row **f** in Table 5. In the -10 to -17 kcal/mol energy range in Table 5, the NO_3-oxidized α-pinene $R'O_2$ and OH-oxidized β-pinene RO_2 in row **g** are both less favorable isomers (2.8 kcal/mol and 2 kcal/mol higher than the most favorable NO_3-oxidized α-pinene and OH-oxidized-β-pinene RO_2s, respectively), translating to lower overall ΔGs. In row **h**, in addition to the OH-oxidized α-pinene and NO_3-oxidized Δ^3-carene being unfavorable by 1.4 and 2.6 kcal/mol, respectively, relative to their corresponding most favorable RO_2 isomer, the low ΔG can be explained by the low energy of the RO products of the two isomers (the lowest energy OH-oxidized RO isomer in the α-pinene case, and only 0.3 kcal/mol higher than the lowest energy NO_3 oxidized RO isomer in the Δ^3-carene case). Finally, the lowest ΔG was found for the reaction between the two O_3-oxidized β-pinene RO_2s (row **i**) due to the low energy of the corresponding RO product.

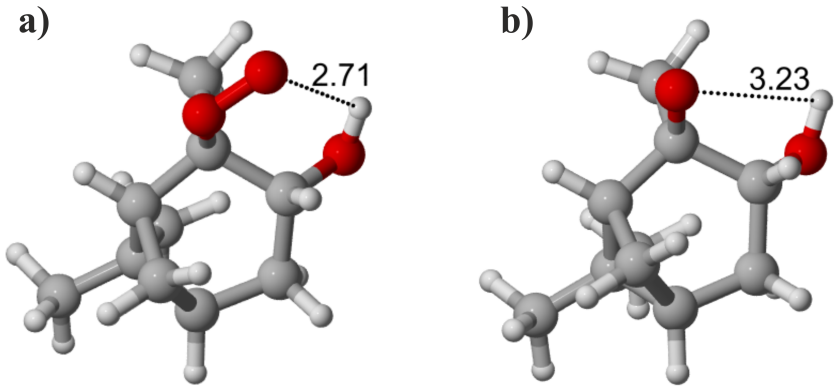

Figure 9: Distances between the OH group and the RO_2 group (a) and the OH group and the RO group (b). The interaction between the OH group and the RO_2 group in (a) translates to a lower RO_2 energy.

Conclusion

Multiple channels compete for RO_2 + HO_2 and RO_2 + RO_2 reactions. The thermodynamics of the two radical propagation reactions involving monoterpene derived RO_2s were studied here. This is the first time such a study has been carried out for a large set of atmospherically relevant monoterpenes and oxidants. The reaction in Gibbs energies were exergonic for all cases. However, the RO_2 + HO_2 $\rightarrow$ RO + OH + O_2 channel (reaction 2) was found to be only barely so for some of the OH and the NO_3 oxidized systems, especially for the lowest-energy RO_2 isomers. Using our simple "rule of thumb" that the reaction Gibbs energy cannot be much higher than -4 kcal/mol for reaction 2 to be competitive, we can rule out this reaction for most OH and NO_3–derived first generation monoterpene RO_2 isomers. However, for each monoterpene-oxidant combination except limonene + OH, at least one RO_2 isomer can be found for which the Gibbs energy of reaction 2 is around or below -4 kcal/mol. These RO_2 isomers could thus conceivably have non-negligible yields for reaction 2. The ozone-derived RO_2s, especially from β-pinene, have somewhat lower reaction Gibbs energies, and for many of their isomers reaction 2 may be feasible.

The $R'O_2 + RO_2 \rightarrow R'O + RO + O_2$ reaction (reaction 5) Gibbs energies varied from a maximum of ∼-3 kcal/mol for the α-pinene-OH system to a minimum of ∼-17 kcal/mol for the β-pinene-O_3 system. The structure of the reactant RO_2 and the product RO strongly affect the reaction Gibbs energies. $RO_2 + RO_2$ self-reaction rates as low as 3×10^{-17} cm^3 $molecule^{-1}$ s^{-1} have been observed for systems similar to those studied here (tertiary $C_4H_9O_2$ radical, in this case).[61] Assuming that the overall mechanism proposed by Ghigo et al.[60] and Lee et al.[54] for $RO_2 + RO_2$ reactions is correct, all RO_2s studied here should have self-reaction rates faster than the slowest observed rate. We can qualitatively conclude, however, that O_3 -derived monoterpene RO_2 are generally likely to have higher, and OH-derived RO_2 lower, overall self- and cross-reaction rates, with NO_3-derived RO_2 representing an intermediate case between the other two.

Supporting information

The Supporting Information is available free of charge via the Internet at http://pubs.acs.org/ and includes reaction Gibbs energies for the studied reactions for all isomers. Output files (.log and .out) for all studied systems are provided in a zip file archived at: https://doi.org/10.5281/zenodo.1476995

Acknowledgements

SI, HR, MPR and TK thank the Academy of Finland (266388,299574), and KHM and HGK thank the Danish Center for Scientific Computing for the financial support. We also thank the CSC IT Center for Science in Espoo, Finland for computing resources.

References

(1) Ehn, M.; Thornton, J. A.; Kleist, E.; Sipilä, M.; Junninen, H.; Pullinen, I.; Springer, M.; Rubach, F.; Tillmann, R.; Lee, B.; et al. A Large Source of Low-Volatility Secondary Organic Aerosol. *Nature* **2014**, *506*, 476-479.

(2) Mentel, T. F.; Springer, M.; Ehn, M.; Kleist, E.; Pullinen, I.; Kurtén, T.; Rissanen, M.; Wahner, A.; Wildt, J. Formation of Highly Oxidized Multifunctional Compounds: Autoxidation of Peroxy Radicals Formed in the Ozonolysis of Alkenes - Deduced from Structure-Product Relationships. *Atmos. Chem. Phys.* **2015**, *15*, 6745-6765.

(3) Berndt, T.; Richters, S.; Kaethner, R.; Voigtländer, J.; Stratmann, F.; Sipilä, M.; Kulmala, M.; Herrmann, H. Gas-Phase Ozonolysis of Cycloalkenes: Formation of Highly Oxidized RO_2 Radicals and Their Reactions With NO, NO_2, SO_2, and Other RO_2 Radicals. *J. Phys. Chem. A* **2015**, *41*, 10336-10348.

(4) Rissanen, M. P.; Kurtén, T.; Sipilä, M.; Thornton, J. A.; Kangasluoma, J.; Sarnela, N.; Junninen, H.; Jørgensen, S.; Schallhart, S.; Kajos, M. K.; et al. The Formation of Highly Oxidized Multifunctional Products in the Ozonolysis of Cyclohexene. *J. Am. Chem. Soc.* **2014**, *136*, 15596-15606.

(5) IPCC, 2013: Climate Change 2013: The Physical Science Basis. Contribution of Working Group I to the Fifth Assessment Report of the Intergovernmental Panel on Climate Change [Stocker, T.F., D. Qin, G.-K. Plattner, M. Tignor, S.K. Allen, J. Boschung, A. Nauels, Y. Xia, V. Bex, P.M. Midgley (eds.)]. Cambridge University Press, Cambridge, United Kingdom and New York, NY, USA, 1535 pp, doi:10.1017/CBO9781107415324.

(6) Sindelarova, K.; Granier, C.; Bouarar, I.; Guenther, A.; Tilmes, S.; Stavrakou, T.; Müller, J.-F.; Kuhn, U.; Stefani, P.; Knorr, W. Global Data Set of Biogenic VOC Emissions Calculated by the MEGAN Model Over the Last 30 Years. *Atmos. Chem. Phys.* **2014**, *14*, 9317-9341.

(7) Crounse, J. D.; Nielsen, L. B.; Jørgensen, S.; Kjaergaard, H. G.; Wennberg, P. O. Autoxidation of Organic Compounds in the Atmosphere. *J. Phys. Chem. Lett.* **2013**, *4*, 3513-3520.

(8) Kurtén, T.; Rissanen, M. P.; Mackeprang, K.; Thornton, J. A.; Hyttinen, N.; Jørgensen, S.; Ehn, M.; Kjaergaard, H. G. Computational Study of Hydrogen Shifts and Ring-Opening Mechanisms in α-Pinene Ozonolysis Products. *J. Phys. Chem. A* **2015**, *119*, 11366-11375.

(9) Atkinson, R. Gas-Phase Tropospheric Chemistry of Volatile Organic Compounds: 1. Alkanes and Alkenes. *J. Phys. Chem. Ref. Data* **1997**, *26*, 215-290.

(10) Park, J.; Jongsma, C. G.; Zhang, R.; North, S. W. OH/OD Initiated Oxidation of Isoprene in the Presence of O_2 and NO. *J. Phys. Chem. A* **2004**, *108*, 10688-10697.

(11) Cabañas, B.; Salgado, S.; Ballesteros, B.; Martínez, E. An Experimental Study on the Temperature Dependence for the Gas-Phase Reactions of NO_3 Radical with a Series of Aliphatic Aldehydes. *J. Atmos. Chem.* **2001**, *40*, 23-39.

(12) Doussin, J. F.; Picquet-Varrault, B.; Durand-Jolibois, R.; Loirat, H.; Carlier, P. A Visible and FTIR Spectrometric Study of the Nighttime Chemistry of Acetaldehyde and PAN Under Simulated Atmospheric Conditions. *J. Photochem. Photobio. A* **2003**, *157*, 283-293.

(13) Ng, N. L.; Brown, S. S.; Archibald, A. T.; Atlas, E.; Cohen, R. C.; Crowley, J. N.; Day, D. A.; Donahue, N. M.; Fry, J. L.; Fuchs, H. F.; et al. Nitrate Radicals and Biogenic Volatile Organic Compounds: Oxidation, Mechanisms, and Organic Aerosol. *Atmos. Chem. Phys.* **2017**, *17*, 2103-2162.

(14) Day, D. A.; Liu, S.; Russell, L. M.; Ziemann, P. J. Organonitrate Group Concentrations in Submicron Particles With High Nitrate and Organic Fractions in Coastal Southern California. *Atmos. Env.* **2010**, *44*, 1970-1979.

(15) Lee, B. H.; Mohr, C.; Lopez-Hilfiker, F. D.; Lutz, A.; Hallquist, M.; Lee, L.; Romer, P.; Cohen, R. C.; Iyer, S.; Kurtén, T.; et al. Highly Functionalized Organic Nitrates in the Southeast United States: Contribution to Secondary Organic Aerosol and Reactive Nitrogen Budgets. *P. Natl. Acad. Sci.* **2016**, *113*, 1516-1521.

(16) Monge-Palcious, M.; Rissanen, M. P.; Wang, Z.; Sarathy, S. M. Theoretical Kinetic Study of the Formic Acid Catalyzed Criegee Intermediate Isomerization: Multistructural Anharmonicity and Atmospheric Implications. *Phys. Chem. Chem. Phys.* **2018**, *20*, 10806-10814.

(17) Orlando, J. J.; Tyndall, G. S. Laboratory Studies of Organic Peroxy Radical Chemistry: An Overview with Emphasis on Recent Issues of Atmospheric Significance. *Chem. Soc. Rev.* **2012**, *41*, 6294-6317.

(18) Orlando, J. J.; Tyndall, G. S.; Wallington, T. J. The Atmospheric Chemistry of Alkoxy Radicals. *Chem. Rev.* **2003**, *103*, 4657-4689.

(19) Hasson, A. S.; Tyndall, G. S.; Orlando, J. J.; Singh, S.; Hernandez, S. Q.; Cambell, S.; Ibarra, Y. Branching Ratios For the Reaction of Selected Carbonyl-Containing Peroxy Radicals With Hydroperoxy Radicals. *J. Phys. Chem. A* **2012**, *116*, 6264-6281.

(20) Vereecken, L.; Peeters, J. Decomposition of Substituted Alkoxy Radicals - Part I: A Generalized Structure-Activity Relationship for Reaction Barrier Heights. *Phys. Chem. Chem. Phys.* **2009**, *11*, 9062-9074.

(21) Dames, E. E.; Green, W. H. The Effect of Alcohol and Carbonyl Functional Groups on the Competition between Unimolecular Decomposition and Isomerization in C_4 and C_5 Alkoxy Radicals. *Int. J. Chem. Kinet.* **2016**, *48*, 544-555.

(22) Hasson, A. S.; Tyndall, G. S.; Orlando, J. J. A Product Yield Study of the Reaction o HO_2 Radicals with Ethyl Peroxy ($C_2H_5O_2$), Acetyl Peroxy ($CH_3C(O)O_2$), and Acetonyl Peroxy ($CH_3C(O)CH_2O_2$) Radicals. *J. Phys. Chem. A* **2004**, *108*, 5979-5989.

(23) Hasson, A. S.; Kuwata, K. T.; Arroyo, M. C.; Petersen, E. B. Theoretical Studies of the Reaction of Hydroperoxy Radicals (HO_2) With Ethyl Peroxy ($CH_3CH_2O_2$), Acetyl Peroxy ($CH_3C(O)O_2$), and Acetonyl Peroxy ($CH_3C(O)CH_2O_2$) Radicals. *J. Photochem. Photobiol. A* **2005**, *176*, 218-230.

(24) Jokinen, T.; Berndt, T.; Makkonen, R.; Kerminen V. -M.; Junninen, H.; Paasonen P.; Stratmann, F.; Herrmann, H.; Guenther, A. B.; Worsnop, D. R. et al. Production of Extremely Low Volatile Organic Compounds from Biogenic Emissions: Measured Yields and Atmospheric Implications. *Proc. Natl. Acad. Sci.* **2015**, *112*, 7123-7128.

(25) Iyer, S.; He, X.; Hyttinen, N.; Kurtén, T.; Rissanen, M. Computational and Experimental Investigation of the Detection of HO_2 Radical and the Products of Its Reaction with Cyclohexene Ozonolysis Derived RO_2 Radicals by an Iodide-Based Chemical Ionization Mass Spectrometer. *J. Phys. Chem. A* **2017**, *121*, 6778-6789.

(26) Hyttinen, N.; Knap, H. C.; Rissanen, M. P.; Jørgensen, S.; Kjaergaard, H. G.; Kurtén, T. Unimolecular HO_2 Loss from Peroxy Radicals Formed in Autoxidation Is Unlikely under Atmospheric Conditions. *J. Phys. Chem. A* **2016**, *120*, 3588-3595.

(27) Halgren, T. A. Merck Molecular Force Field. I. Basis, Form, Scope, Parameterization, and Performance of MMFF94. *J. Comput. Chem.* **1996**, *17*, 490-519.

(28) Halgren, T. A. Merck Molecular Force Field. II. MMFF94 van der Waals and Electrostatic Parameters for Intermolecular Interactions. *J. Comput. Chem.* **1996**, *17*, 520-552.

(29) Halgren, T. A. Merck Molecular Force Field. III. Molecular Geometries and Vibrational Frequencies for MMFF94. *J. Comput. Chem.* **1996**, *17*, 553-586.

(30) Halgren, T. A.; Nachbar, R. B. Merck Molecular Force Field. IV. Conformational Energies and Geometries for MMFF94. *J. Comput. Chem.* **1996**, *17*, 587-615.

(31) Halgren, T. A. Merck Molecular Force Field. V. Extension of MMFF94 Using Experimental Data, Additional Computational Data, and Empirical Rules. *J. Comput. Chem.* **1996**, *17*, 616-641.

(32) Halgren, T. A. MMFF VII. Characterization of MMFF94, MMFF94s, and Other Widely Available Force Fields for Conformational Energies and for Intermolecular-Interaction Energies and Geometries. *J. Comput. Chem.* **1999**, *20*, 730-748.

(33) Becke, A. D. Density-Functional Thermochemistry. III. The Role of Exact Exchange. *J. Chem. Phys.* **1993**, *98*, 5648-5652.

(34) Lee, C.; Yang, W.; Parr, R. H. Development of the Colle-Salvetti Correlation-Energy Formula Into a Functional of the Electron Density. *Phys. Rev. B* **1988**, *37*, 785-789.

(35) Hehre, W. J.; Ditchfield, R.; Pople, J. A. Self-Consistent Molecular Orbital Methods. XII. Further Extensions of Gaussian-Type Basis Sets for Use in Molecular Orbital Studies of Organic Molecules. *J. Chem. Phys.* **1972**, *56*, 2257-2261.

(36) Clark, T.; Jayaraman, C.; Spitznagel, G. W.; Schleyer, P. v. R. Efficient Diffuse Function-Augmented Basis Sets for Anion Calculations. III. The 3-21+G Basis Set for First-Row Elements, Li-F. *J. Comput. Chem.* **1983**, *4*, 294-301.

(37) Frisch, M. J.; Pople, J. A.; Stephen, B. J. Self-Consistent Molecular Orbital Methods 25. Supplementary Functions for Gaussian Basis Sets. *J. Chem. Phys.* **1984**, *80*, 3265-3269.

(38) Møller, K. H.; Otkjaer, R. V.; Hyttinen, N.; Kurtén, T.; Kjaergaard, H. G. Cost-Effective Implementation of Multiconformer Transition State Theory for Peroxy Radical Hydrogen Shift Reactions. *J. Phys. Chem. A* **2016**, *120*, 10072-10087.

(39) Spartan '14; Wavefunction Inc: Irvine CA, 2014.

(40) Spartan '16; Wavefunction Inc: Irvine CA, 2016.

(41) Hyttinen, N.; Rissanen, M. P.; Kurtén, T. Computational Comparison of Acetate and Nitrate Chemical Ionization of Highly Oxidized Cyclohexene Ozonolysis Intermediates and Products. *J. Phys. Chem. A* **2017**, *121*, 2172-2179.

(42) Chai, J. D.; Head-Gordon, M. Long-Range Corrected Hybrid Density Functionals with Damped Atom-Atom Dispersion Corrections. *Phys. Chem. Chem. Phys.* **2008**, *10*, 6615-6620.

(43) Dunning, T. H. Gaussian Basis Sets for Use in Correlated Molecular Calculations. I. The Atoms Boron Through Neon and Hydrogen. J. Chem. Phys. 1989, 90, 1007-1023.

(44) Kendall, R. A.; Dunning, T. H.; Harrison, R. J. Electron Affinities of the First-Row Atoms Revisited. Systematic Basis Sets and Wave Functions. J. Chem. Phys. 1992, 96, 6796-6806.

(45) Frisch, M. J.; Trucks, G. W.; Schlegel, H. B.; Scuseria, G. E.; Robb, M. A.; Cheeseman, J. R.; Scalmani, G.; Barone, V.; Mennuci, B.; Petersson, G. A.; et al. *Gaussian 09*. Revision D.01, Gaussian, Inc.: Wallingford, CT, 2009.

(46) Partanen, L.; Vehkamäki, H.; Hansen, K.; Elm, J.; Henschel, H.; Kurtén, T.; Halonen, R.; Zapadinsky, E. Effect of Conformers on Free Energies of Atmospheric Complexes. *J. Phys. Chem. A* **2016**, *120*, 8613-8624.

(47) Riplinger, C. Neese, F. An Efficient and Near Linear Scaling Pair Natural Orbital Based Local Coupled Cluster Method. *J. Chem. Phys.* **2013**, *138*, 034106.

(48) Neese, F. The ORCA Program System. *Wiley Interdiscip. Rev. Comput. Mol. Sci.* **2012**, *2*, 73-78.

(49) Minenkov, Y.; Wang, H.; Wang, Z.; Sarathy, S. M.; Cavallo, L. Heats of Formation of Medium-Sized Organic Compounds from Contemporary Electronic Structure Methods. *J. Chem. Theory Comput.* **2017**, *13*, 3537-3560.

(50) Montgomery, J. A. Jr.; Frisch, M. J. A Complete Basis Set Model Chemistry. VI. Use Of Density Functional Geometries and Frequencies. *J. Chem. Phys.* **1999**, *110*, 2822-2827.

(51) Peverati, R.; Truhlar, D. G. Improving the Accuracy of Hybrid Meta-GGA Density Functionals by Range Separation. *J. Phys. Chem. Lett.* **2011**, *2*, 2810-2817.

(52) Ditchfield, R.; Hehre, W. J.; Pople, J. A. Self-Consistent Molecular Orbital Methods. IX. An Extended Gaussian-Type Basis for Molecular-Orbital Studies of Organic Molecules. *J. Chem. Phys.* **1971**, *54*, 724-728.

(53) Hariharan, P. C.; Pople, J. A. The Influence of Polarization Functions on Molecular Orbital Hydrogenation Energies. *Theor. Chem. Acc.* **1973**, *28*, 213-222.

(54) Lee, R.; Grynova, G.; Ingold, K. U.; Coote, M. L. Why Are Sec-Alkylperoxyl Bimolecular Self-Reactions Orders of Magnitude Faster Than the Analogous Reactions of Tert-Alkylperoxyls? The Unanticipated Role of CH Hydrogen Bond Donation. *Phys. Chem. Chem. Phys.* **2016**, *18*, 23673.

(55) Rio, C.; Flaud, P.-M.; Loison, J.-C.; Villenave, E. Experimental Revaluation of the Importance of the Abstraction Channel in the Reactions of Monoterpenes with OH Radicals. *Chem. Phys. Chem.* **2010**, *11*, 3962-3970.

(56) Atkinson, R.; Arey, J. Gas-Phase Tropospheric Chemistry of Biogenic Volatile Organic Compounds: A Review. *Atmos. Environ.* **2003**, *37*, 197-219.

(57) Ham, J. E.; Harrison, J. C.; Jackson, S. R.; Wells, J. R. Limonene Ozonolysis in the Presence of Nitric Oxide: Gas-Phase Reaction Products and Yields. *Atmos. Environ.* **2016**, *132*, 300-308.

(58) Boyd, A. A.; Flaud, P.-M.; Daugey, N.; Lesclaux, R. Rate Constants for RO_2 + HO_2 Reactions Measured Under a Large Excess of HO_2. *J. Phys. Chem. A* **2003**, *6*, 818-821.

(59) Nguyen, T. L.; Peeters, J.; Vereecken, L. Theoretical Study of the Gas-Phase Ozonolysis of β-Pinene ($C_{10}H_{16}$. *Phys. Chem. Chem. Phys.* **2009**, *11*, 5643-5656.

(60) Ghigo, G.; Maranzana, A.; Tonachini, G. Combustion and Atmospheric Oxidation of Hydrocarbons: Theoretical Study of the Methyl Peroxyl Self-Reaction. *J. Chem. Phys.* **2003**, *118*, 10575-10583.

(61) Shallcross, D. E.; Raventos-Duran, M. T.; Bardwell, M. W.; Bacak, A.; Solman, Z.; Percival, C. J. A Semi-Emperical Correlation for the Rate Coefficients for Cross- and Self-Reactions of Peroxy Radicals in the Gas-Phase. *Atmos. Env.* **2005**, *39*, 763-771.

TOC Graphic